

N -body models of extended star clusters

Jarrold R. Hurley^{1*}, A. Dougal Mackey²

¹*Centre for Astrophysics and Supercomputing, Swinburne University of Technology, P.O. Box 218, VIC 3122, Australia*

²*Research School of Astronomy & Astrophysics, The Australian National University, Mount Stromlo Observatory, Cotter Road, Weston Creek, ACT 2611, Australia*

Accepted 2010 Month xx. Received 2010 Month xx; in original form 2010 May 7

ABSTRACT

We use direct N -body simulations to investigate the evolution of star clusters with large size-scales with the particular goal of understanding the so-called extended clusters observed in various Local Group galaxies, including M31 and NGC 6822. The N -body models incorporate a stellar mass function, stellar evolution and the tidal field of a host galaxy. We find that extended clusters can arise naturally within a weak tidal field provided that the tidal radius is filled at the start of the evolution. Differences in the initial tidal filling-factor can produce marked differences in the subsequent evolution of clusters and the size-scales that would be observed. These differences are more marked than any produced by internal evolution processes linked to the properties of cluster binary stars or the action of an intermediate-mass black hole, based on models performed in this work and previous work to date. Models evolved in a stronger tidal field show that extended clusters cannot form and evolve within the inner regions of a galaxy such as M31. Instead our results support the suggestion many extended clusters found in large galaxies were accreted as members of dwarf galaxies that were subsequently disrupted. Our results also enhance the recent suggestion that star clusters evolve to a common sequence in terms of their size and mass.

Key words: stellar dynamics— methods: N -body simulations— stars: evolution— globular clusters: general— galaxies: star clusters

1 INTRODUCTION

Recent observations have unearthed a new class of extragalactic objects which have been termed extended star clusters. These have shown up in the outer regions of a range of galaxy types: spirals M31 (Huxor et al. 2005; Mackey et al. 2006; Huxor et al. 2008) and M33 (Stonkutė et al. 2008; Huxor et al. 2009), the dwarf irregular NGC 6822 (Hwang et al. 2005; Huxor et al. 2010b) and the Sculptor Group dwarf elliptical Scl-dE1 (Sc22: Da Costa et al. 2009). The few extended clusters (ECs) for which high quality colour-magnitude diagrams (CMDs) are available appear old and metal-poor with no evidence for multiple populations (Mackey et al. 2006). Thus they have similar stellar populations to those of typical Milky Way and M31 globular clusters (GCs). A faint extended cluster in the giant elliptical galaxy NGC 5128 has also recently been discovered (Mouhcine et al. 2010) with properties similar to the Palomar GCs found in the outer regions of the Milky Way (van den Bergh & Mackey 2004).

The size scales of the ECs, generally measured as the projected half-light radius, $r_{h,l}$ (where we will use the three-

dimensional r_h for the related half-mass radius), are in the range of 10 – 35 pc which places them between regular globular clusters and low-luminosity dwarf spheroidal galaxies (Huxor et al. 2005; Da Costa et al. 2009). As such these objects raise questions as to whether they are star clusters that have somehow evolved to much larger radii than is typical for Milky Way globular clusters or if they are more closely associated with dwarf spheroidals, perhaps even to the extent of possessing some kind of dark matter component. Interestingly there are extended clusters in M31 with the same luminosity, and at the same distance from the centre of the galaxy, R_{gc} , as regular globular clusters but with a half-light radius a factor of ten or more greater (Huxor et al. 2010a). If the extended clusters are indeed a sub-class of globular cluster then we must ask how clusters that appear very similar in many respects can obtain quite distinct structural properties.

In the case of two clusters of the same mass M at the same R_{gc} but with markedly different half-mass radii we must consider the prior r_h history of both clusters, possibly traced back to having distinct initial r_h values. In turn this may indicate different modes of cluster formation (Elmegreen 2008; Da Costa et al. 2009). Baumgardt & Kroupa (2007) have shown that variations in star for-

* E-mail: jhurley@swin.edu.au (JRH)

mation efficiency for clusters as they form from molecular clouds can lead to a range of initial half-mass radii. One of the goals of this paper is to investigate the ramifications of this for the long-term structural evolution of realistic star cluster models. In particular we would like to know if large differences in the structure of clusters at a Hubble time is more likely a result of different structures at birth, different internal evolution histories (e.g. formation of binaries) or possibly having experienced different external environments in the past. Of course a combination of these effects is also possible. We are also interested generally in producing N -body models of potential extended star clusters.

In general terms the evolution of a star cluster is dictated by internal processes, primarily two-body relaxation, as well as the influence of the gravitational potential of the host galaxy. Historically the gross properties, such as the dissolution time, have been described in terms of R_{gc} , M and r_{h} (Fall & Rees 1977; Gnedin & Ostriker 1997). The first two can be used to define a tidal radius, r_{t} , while the timescale for two-body relaxation can be derived from the latter two quantities. Typically the timescale on which stars are pushed across the tidal boundary and the cluster subsequently evaporates owing to two-body relaxation can be estimated from M and r_{h} as well (see Gnedin, Lee & Ostriker 1999 for a discussion) although as shown by Gieles & Baumgardt (2008) the tidal field strength is the most important factor in determining mass-loss rates. For clusters orbiting in the inner regions of a galaxy the lifetime can also be affected by gravitational shocks from the disk and/or bulge of the galaxy (Gnedin & Ostriker 1997). If we assume that the half-mass radius of a cluster scales with the tidal radius, as is often done (and noting that r_{t} decreases with time), then two clusters of the same mass at the same R_{gc} will have the same r_{h} . In this picture any differences in r_{h} (assuming the clusters are the same age) requires that the masses in fact be different or that the clusters have followed different evolutionary paths. It may be possible that both clusters did not always reside at R_{gc} , having different galactic orbits, with the extreme scenario being that one cluster was accreted during a galaxy merger (Mackey & Gilmore 2004; Da Costa et al. 2009). Another possibility is that internal factors such as the fraction of binaries (Gao et al. 1991) or the formation of an intermediate-mass black hole (Kormendy & Richstone 1995) played a role. Prior N -body models that have documented the effect of such factors on the evolution of a star cluster include Giersz & Heggie (1997), de la Fuente Marcos (1997), Portegies Zwart et al. (2001), Baumgardt, Makino & Hut (2005) and Mackey et al. (2008).

We will be looking at the evolution of N -body models that start with different sizes and models that evolve in tidal fields of different strength. For the latter we have in mind M31 and NGC 6822 as examples of galaxies imposing a strong and weak galactic tidal field, respectively. We will be interested in the maximum half-mass (and half-light) radii that can be obtained at the same R_{gc} in these two galaxy types. In particular, we choose $R_{\text{gc}} = 10$ kpc. This is motivated by the location of the ECs in NGC 6822 which extend out to 10.8 kpc in projection from the galaxy centre (Hwang et al. 2005; Huxor et al. 2010b) as well as the observation of ECs and GCs of similar luminosity/mass at about this position in M31. This radius could be considered an extreme choice for M31 which has both ECs and GCs out

to at least 100 kpc in projection (Martin et al. 2006, Huxor et al. 2008, Huxor et al. 2010c), with only the innermost presently-known ECs residing at ~ 10 kpc; however, selecting this radius for our M31 models will give an indication of the maximum expected influence of a strong tidal field on EC evolution. Note also that our models should encompass the situation for additional ECs such as the two known in M33, which reside in a galaxy intermediate in mass between M31 and NGC 6822 but again at comparable radii: 12.4 and 28.6 kpc in projection, respectively (Huxor et al. 2009). In this sense we expect our results to be quite widely applicable.

The remainder of this paper is structured as follows. In Section 2 we describe the setup of the N -body models, including the N -body software and how the tidal field is modelled. This is followed by the results in Section 3 and a discussion of the implications for observations of ECs in Section 4.

2 MODELS

The model clusters in this work are evolved using the **NBODY6** direct N -body code (Aarseth 2003). Gravitational forces are computed using a fourth-order Hermite integration scheme, without softening, on either standard CPU or graphics processing unit (GPU) hardware. **NBODY6** is the sister code to **NBODY4** which instead interfaced with GRAPE-6 hardware (Makino 2002) for rapid force calculation. The codes include algorithms for stellar and binary evolution as described in Hurley (2008a, 2008b) and deal directly with the effects of close dynamical encounters: perturbations to binary orbits, collisions and mergers, formation of three- and four-body subsystems, exchange interactions, tidal capture and binary disruption.

We focus on a set of models starting with $N = 100\,000$ particles (stars or binaries). Each model includes a mass function, stellar evolution and the tidal field of a parent galaxy. Single star masses are taken from the initial mass function (IMF) of Kroupa, Tout & Gilmore (1993) between the limits of $0.1 - 30 M_{\odot}$. When including binary stars the masses of two randomly chosen single stars are combined and then reassigned using a mass-ratio from a uniform distribution in order to give the primary and secondary masses. Initial periods are drawn from the log-normal distribution determined by Duquennoy & Mayor (1991) from observations of local solar-type stars and the eccentricities are assumed to follow a thermal distribution (Heggie 1975). Metallicity is set at $Z = 0.001$ for the stars. The initial positions and velocities are assigned according to a either a Plummer density profile (Plummer 1911; Aarseth, Hénon & Wielen 1974) or a King model (King 1966: $W_0 = 7$) with the stars in virial equilibrium.

The influence of the tidal field of the parent galaxy is modelled by assuming that the model cluster follows a circular orbit at distance R_{gc} from a point-mass galaxy of mass M_{g} . At this stage we are not interested in the complicating factors presented by more realistic three-dimensional galaxy potentials. The implications of this decision will be discussed in Section 4. The relevant equations of motion are developed by linearizing the galactic potential in a rotating reference frame centered on the cluster centre-of-mass with the x -axis

directed away from the galactic centre and the *y*-axis in the direction of motion (see Giersz & Heggie 1997; Vesperini & Heggie 1997). A tidal radius (also called the Jacobi radius: Gieles & Baumgardt 2008),

$$r_t = (M/3M_g)^{1/3} R_{gc}, \quad (1)$$

can then be defined corresponding to the saddle point on the *x*-axis of the effective cluster potential. Within an *N*-body simulation the user has the freedom to set a length-scale R_{sc} with one possible choice being that the outermost stars of the initial density profile are scaled to sit at r_t , in which case the cluster is said to be Roche-lobe filling (e.g. Tanikawa & Fukushige 2005). The Plummer profile formally extends to infinite radius so in practice a cut-off at a radius of $\sim 10 r_h$ is applied to avoid rare cases of large distance. For our Plummer models described below this leads to $r_{max} \simeq 8 r_h$, where r_{max} is the position of the outermost star, and we define r_{max}/r_t as the tidal-radius filling factor. The related ratio r_h/r_t is an important quantity to describe the structure of star cluster models.

In this work we model parent galaxies with two distinct masses: $M_g = 9 \times 10^9 M_\odot$ to represent a dwarf galaxy such as NGC 6822 and $M_g = 9 \times 10^{10} M_\odot$ to model a more substantial galaxy such as M31. As discussed above all clusters are set to orbit at $R_{gc} = 10$ kpc in these model galaxies.

Six distinct models are performed. These are listed in Table 1. Models N1, N2 and N3 are all evolved in the NGC 6822-like tidal field. They are identical in all respects except for using $R_{sc} = 7, 14$ and 21 so that they have initial tidal-radii filling factors of 0.33, 0.66 and 1.00, respectively (the corresponding r_h/r_t ratios are given in Table 1). Model N2b is the same as N2 except that it starts with 95 000 single stars and 5 000 binaries rather than 100 000 single stars. We then have Model M1 which is evolved in the stronger M31-like tidal field for comparison. All of these models start with a Plummer density profile whereas Model M2 starts with a King profile and is also evolved in the M31-like tidal field. Both M1 and M2 start with tidal-radii filling factors of 1.00 (r_{max} matches the tidal radius). The initial mass of each model is $M \simeq 58 000 M_\odot$ which gives an initial r_t of 129 pc for models N1, N2, N2b and N3 compared to 60 pc for models M1 and M2. Each model is evolved to an age of 20 Gyr or until 5% of the stars remain, whichever occurs first – the latter only happens for M2 at an age of 17.4 Gyr. The simulations are performed using Tesla S1070 GPUs at Swinburne University.

We will also lean on the results of some previous *N*-body simulations when evaluating our results. These include models K100-00a and K100-00b of Hurley (2007) which both featured 100 000 single stars evolved within a standard Galactic tidal field (Giersz & Heggie 1997): an orbital speed of 220 km s^{-1} at $R_{gc} = 8.5$ kpc (with corresponding $M_g = 9 \times 10^{10} M_\odot$). The two models were setup in the same way and the difference of note was the formation of a long-lived binary composed of two stellar-mass black holes (BHs) in K100-00b which altered the central structure of the cluster compared to K100-00a. Along the same lines we will use the results of Mackey et al. (2008) who looked at the effect of a population of BH-BH binaries on cluster evolution, as well as models including intermediate-mass black-holes (e.g. Gill et al. 2008). Also mentioned will be models of 30 000

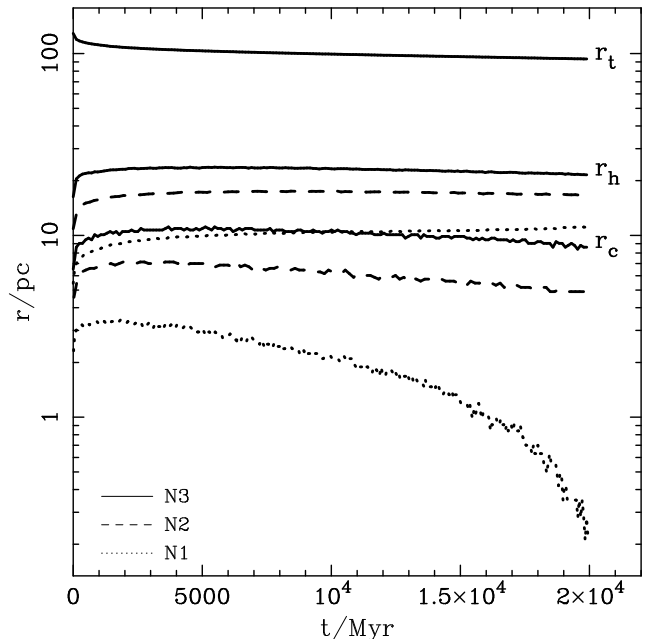


Figure 1. Evolution of the half-mass radius, r_h , and the core radius, r_c , for the NGC 6822 models N1 (dotted lines), N2 (dashed lines) and N3 (solid lines) noting that r_c is always less than r_h . The tidal radius of model N3 is also shown.

single stars from Hurley et al. (2004), mainly for illustrative purposes.

It is important to emphasize that unless otherwise specified the radii quoted will be based on three-dimensional data. The core radius, r_c , comes from a density-weighted calculation (Casertano & Hut 1985) that is traditionally used in *N*-body models and is not comparable to the quantity derived by observational methods. This has been discussed in the past (e.g. Wilkinson et al. 2003; Hurley 2007). For our purposes this is fine as we use r_c as an indicator of the cluster dynamical state, in particular to determine if core-collapse has been reached, rather than to compare to observed results for actual clusters. We also use r_h as the three-dimensional half-mass radius. Here we are mainly interested in the relative values between models. However, we will also provide the half-light radius, $r_{h,1}$, calculated from a two-dimensional projection of the data, to give a reference point for comparing the size of the model clusters to real clusters.

3 RESULTS

The different initial filling factors of models N1, N2 and N3 lead to different initial half-mass radii (see Table 1) and allow us to investigate the effect this has on the long-term evolution of star clusters residing within a weak tidal field. It is well established that the evolution of a star cluster is intricately linked to the two-body relaxation timescale which is typically characterized by the value at the half-mass radius,

$$t_{rh} \propto \frac{N}{\log 0.4N} \left(\frac{r_h^3}{M} \right)^{1/2} \quad (2)$$

Table 1. Key information for the initial models of the new simulations performed in this work and also the models K100-00a and K100-00b from Hurley (2007). All models started with $N = 100\,000$ stars and $M \simeq 58\,000 M_\odot$. Column 1 gives the label assigned to each model where N represents the NGC 6822-like tidal field and M the M31-like tidal field. In Columns 2 and 3 we show the density profile and the primordial binary fraction, respectively. Columns 4-8 give the half-mass radius, tidal radius, half-mass to tidal radius ratio, tidal radius filling factor and half-mass relaxation timescale at $T = 0$ Gyr. All lengths are in pc units and relaxation times are in Myr.

Label	profile	f_b	r_h	r_t	r_h/r_t	r_{\max}/r_t	T_{rh}
N1	Plum	0.00	5.4	129.0	0.042	0.33	980
N2	Plum	0.00	10.9	129.0	0.084	0.66	2770
N2b	Plum	0.05	10.9	129.0	0.084	0.66	2697
N3	Plum	0.00	16.3	129.0	0.126	1.00	5090
M1	Plum	0.00	7.8	60.0	0.130	1.00	1670
M2	King	0.00	8.7	60.0	0.145	1.00	1990
K100-00a	Plum	0.00	6.6	51.0	0.129	1.00	1440
K100-00b	Plum	0.00	6.6	51.0	0.129	1.00	1430

Table 2. As for Table 1 but now showing properties of the models at $T = 12$ Gyr. Column 1 gives the label assigned to each model. Column 2 gives the half-mass radius followed by an estimate of the error in this value. This is repeated in columns 4 and 5 for the 2-dimensional projected half-light radius. The values in columns 2 and 4 are computed from the average of five snapshots taken over a 300 Myr period centred on 12 Gyr. Errors in columns 3 and 5 are based on the difference between the average and the greatest outlier. Columns 6-8 give the tidal radius, the mass that remains bound within the tidal radius and the half-mass relaxation timescale. All lengths are in pc units, masses in M_\odot and relaxation times are in Myr.

Label	r_h	error	$r_{h,1}$	error	r_t	M	T_{rh}
N1	10.5	± 0.1	5.6	± 1.1	106.0	32 470	3240
N2	17.3	± 0.1	10.5	± 1.0	103.0	29 940	6680
N2b	17.3	± 0.1	11.1	± 1.8	103.0	29 960	6400
N3	23.0	± 0.1	15.4	± 1.0	97.0	25 410	9440
M1	8.1	± 0.2	5.6	± 1.2	38.4	15 430	1410
M2	5.6	± 0.1	3.9	± 1.4	32.5	9 420	620
K100-00a	5.9	± 0.1	4.0	± 1.7	35.4	15 780	890
K100-00b	6.5	± 0.1	3.2	± 0.7	35.2	15 470	1020

(Spitzer 1987; Binney & Tremaine 1987). For a cluster to reach the dynamically-evolved state of core-collapse it has been shown that at least ten half-mass relaxation times must have elapsed (e.g. Baumgardt, Hut & Heggie 2002; Hurley 2007). The half-mass relaxation timescales corresponding to the initial states of the clusters are given in Table 1 for our models. In Table 2 the timescales for the clusters at an age of 12 Gyr are given. We can see that of models N1, N2 and N3 it is only model N1, the initially most compact cluster, that is likely to reach core-collapse within 20 Gyr of evolution. This is borne out in Figure 1 which shows the evolution of r_c and r_h for the three models. The tidal radius of model N3 is also shown for reference. Indeed, model N1 is close to core-collapse when the simulation is stopped at 20 Gyr. By comparison, the core radii of models N2 and N3 are showing no signs of decreasing to the small values associated with core-collapse (at 12 Gyr r_c for N3 is the same size as r_h for N1). Based on the half-mass relaxation timescales such slow evolution for models N2 and N3 is expected as at 20 Gyr they have evolved for less than four and three half-mass relaxation times, respectively.

It can be seen in Figure 1 that for all three models there is an initial rapid phase of increasing r_h . This corresponds to the phase of violent relaxation associated with stellar evolu-

tion mass-loss from massive stars in which there is an overall expansion of the cluster. Afterwards the evolution of r_h proceeds slowly and for models N2 and N3 r_h is effectively constant over Gyr timescales. In model N1 we do see a continual increase in r_h as the outer regions of the cluster expand in response to the shrinking core. At all times r_h for N3 remains larger than for N2 which in turn remains larger than for N1: the initial hierarchy of cluster size is maintained and the initially more extended cluster remains so. It is true that the spread in r_h decreases with age – r_h for N3 is initially a factor of three greater than for N1 compared to a factor of two greater at 20 Gyr – but even so the initial cluster size scale has an important bearing on the subsequent evolution.

As described by Heggie & Hut (2003) an interesting way to understand the evolution of a star cluster is through ratios of the key radii (r_c , r_h and r_t). In Figure 2a we reproduce Fig. 33.2 of Heggie & Hut (2003) and use it to give a basic overview of the expected behaviour (see Ch. 33 of Heggie & Hut 2003 for more background and detail). The evolution paths are distinct for clusters initially contained well within the tidal radius (path A in Fig. 2a) or filling the tidal radius (path B). For the former case all regions of the cluster expand during the initial period of violent relaxation so that $r_c/r_h \sim \text{constant}$ while r_h/r_t increases (as r_t changes

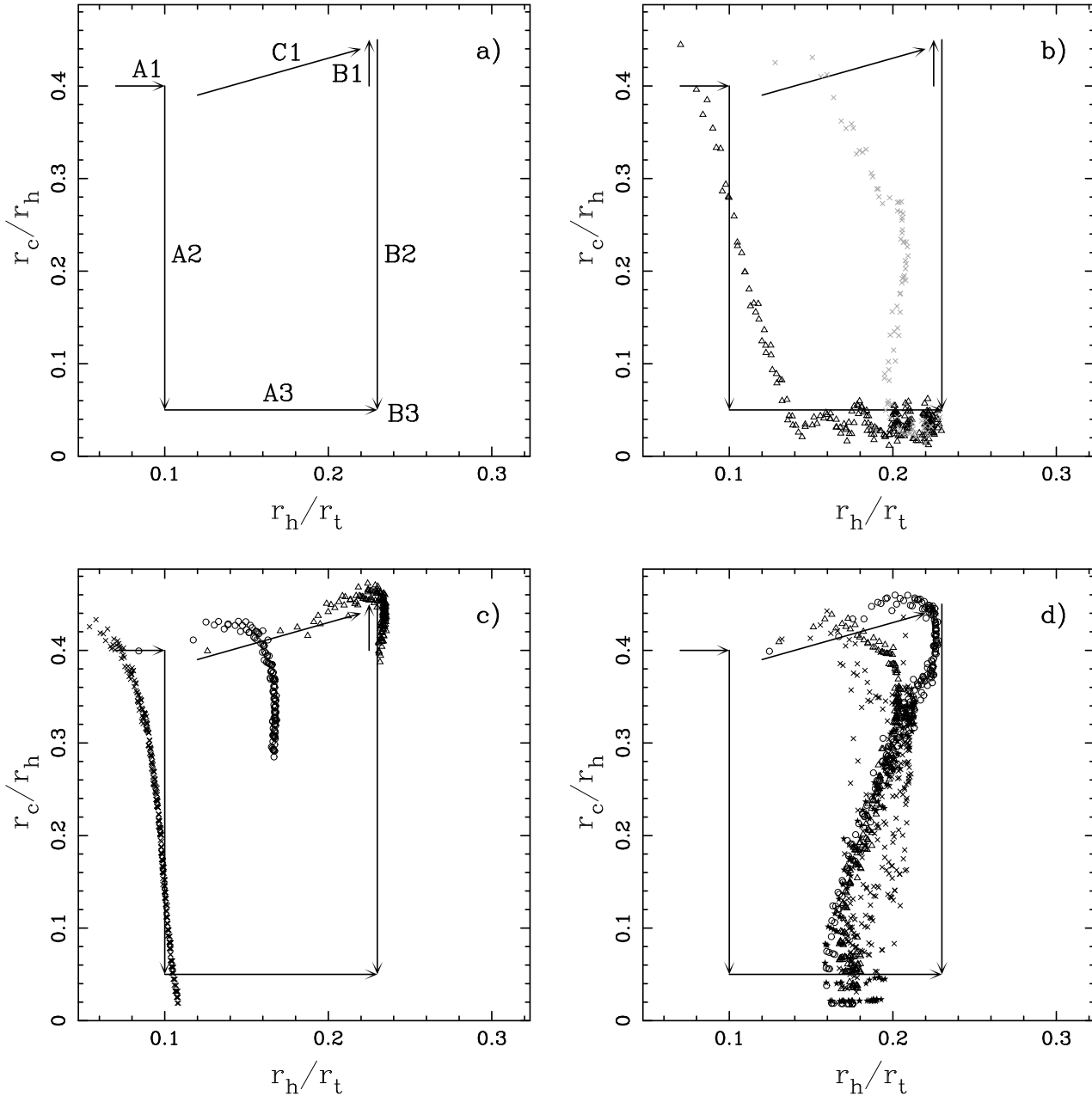


Figure 2. Evolution of star clusters in the r_h/r_t versus r_c/r_h plane. Panel a) is for illustrative purposes (see text for an explanation of the labels) while panel b) shows Models 3 (open triangles) and 7 (grey crosses) of Hurley et al. (2004). In panel c) we show models N1 (crosses), N2 (open circles) and N3 (open triangles) of this work. Finally, panel d) shows models M1 (open circles) and M2 (solid stars) of this work as well as Models K100-00a (open triangles) and K100-00b (crosses) of Hurley (2007).

only minimally). Thus the cluster evolves along path A1. For the tidally-filling cluster, where in the extreme we assume that r_h follows the evolution of r_t , we would instead expect an increase in r_c/r_h while r_h/r_t remains constant (path B1). Following violent relaxation the cluster then enters a long-lived period of dynamical evolution driven by two-body relaxation where mass-segregation develops and the cluster evolves towards core-collapse. During this time r_c decreases markedly, r_h changes only slightly by comparison and r_t decreases slowly. This gives paths A2 and B2 as both regimes head towards low r_c/r_h . Post-collapse evolution is characterized by a central energy source (e.g. hard binaries) heating

the core which will oscillate in size but with a time-average that varies little. For an isolated cluster we would expect r_h to increase during this phase so any cluster that is not yet tidally-filling will move along path A3 to join B3. The tidally-filling clusters are expected to have little evolution in the r_c/r_h - r_h/r_t plane after core-collapse. We can readily verify this by looking at the evolution of some actual models. First we start with two models of $N = 30\,000$ stars from Hurley et al. (2004) where one model started well within r_t and the other started with $r_{\max} = r_t$. These are shown in Figure 2b and we clearly distinguish path A and path B-like evolution before both clusters end at a similar point. In real-

ity we would expect most clusters to evolve between the two extremes of paths A and B as they head towards B3, particularly during violent relaxation where clusters will expand and can move along path C1 to join B2. We see this to some extent when we look at the evolution of models N1, N2 and N3 in Figure 2c. Model N3 in particular first evolves across the phase space before starting down path B2. There is also a clear distinction between the evolution of the three models, residing at well separated r_h/r_t values as they start to move down in r_c/r_h . Of course, owing to the large half-mass relaxation timescales, the models do not get the opportunity to evolve completely through the parameter space.

We have now seen that it is possible to reach large r_h values for clusters evolving in a weak NGC 6822-like tidal field and that quite distinct r_h values can be obtained by clusters with different initial sizes. But can distinct r_h values be obtained by other means? The first possibility we explore is the inclusion of a primordial binary population (Model N2b). Figure 3 compares the r_h evolution of models N2 and N2b which are identical in setup except for a 5 per cent primordial binary population in the latter. We see that the r_h evolution is indistinguishable. This is also true for the evolution of bound cluster mass (see Table 2) and other general quantities. We note that as an accuracy check models N2 and N2b were both performed twice with different initial random number seeds and the variation between different realisations of the same model was less than the difference between the two model types. For these extended clusters it is not surprising that the addition of binaries makes little difference to the evolution. The long relaxation times for Models N2 and N2b (see Tables 1 and 2) mean that the collisional extraction of binding energy from the binary orbits will not be efficient at heating the cluster.

The second possibility for internal evolution creating r_h differences between models relates to the formation of tight BH-BH binaries which then act as a central energy source to heat the cluster. Hurley (2007) showed that the formation of one such long-lived BH-BH binary could double the r_c/r_h ratio compared to a similar model which did not form a BH-BH binary. However, we compare the r_h evolution of these models (K100-00a and K100-00b from Hurley 2007) in Figure 3 (and in Tables 2) and we see no clear distinction. Mackey et al. (2008) took this further and contrasted the evolution of clusters with no BH-BH binaries to that of clusters which retained a large number of post-supernovae BHs (~ 200) that subsequently sank to the cluster centre and formed BH-BH binaries (as many as five such binaries present at any one time). The focus was on star clusters in the Large Magellanic Cloud and as such a tidal field the same as for our NGC 6822 case was used (but with $R_{gc} = 6$ kpc rather than 10 kpc). They found that the inclusion of the BH-BH binaries could increase r_h by as much as a factor of two by the time that the model with no BH-BH binaries had reached core-collapse (compared to a corresponding factor of 20 increase in r_c). The r_h behaviour first started to diverge after 1 – 2 Gyr of evolution, corresponding to roughly one half-mass relaxation time, with the expansion driven on the shorter relaxation timescale of the centralised BH population. However, we note that the most extended of these models were in the advanced stages of dissolution at a Hubble time. Another possibility is one that has gathered much attention of late, namely the question of whether

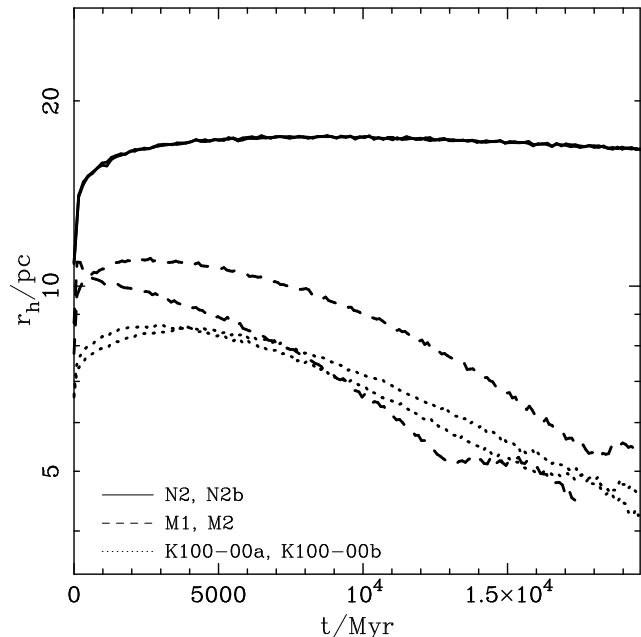


Figure 3. Comparison of the half-mass radius evolution for models N2 and N2b (solid lines), M1 and M2 (dashed lines), and K100-00a and K100-00b (dotted lines) of Hurley (2007).

or not some star clusters harbour intermediate-mass black holes (IMBHs). Gill et al. (2008) compare the r_h evolution of models with and without an IMBH and find no significant difference until well after core-collapse and even at very late times the difference is still less than a factor of two. Baumgardt, Makino & Hut (2005) looked at the effect of increasing IMBH mass and found an increase in r_h of 15 per cent at most. It should be noted that the maximum black hole mass included in the models to date is $1000 M_\odot$ and that the heating produced by significantly more massive IMBHs, if indeed they exist, is yet to be documented.

We next look at the evolution of our models M1 and M2 which were evolved in the stronger M31-like tidal field. These models started with different initial density profiles so provide an opportunity to look at how the choice of a Plummer or King profile affects the r_h evolution. This is shown in Figure 3 (also in Figure 4) and we see that at various stages in the evolution the difference can be up to 50 per cent. The radius evolution of models M1 and M2 is studied in more detail in Figure 4. Comparing this to Figure 1 we clearly see that the stronger tidal field drives more rapid evolution for the M31 models relative to their NGC 6822 counterparts. Indeed, both M1 and M2 reach core-collapse prior to 20 Gyr. The model with the King density profile evolves more rapidly. This is primarily owing to a greater central density of stars in the initial model which led to a greater rate of dynamical interactions, more mass lost across the tidal boundary in the early stages, and consequently a reduced relaxation timescale. However, in the M - r_h plane (Figure 5) the evolution of models M1 and M2 is very similar. Interestingly both M1 and M2 appear to keep r_h approximately constant after core-collapse, behaviour that was noted by Küpper, Kroupa & Baumgardt (2008) in their models. We also see that models M1 and M2, as well as models K100-00a and K100-00b of Hurley (2007) all evolve

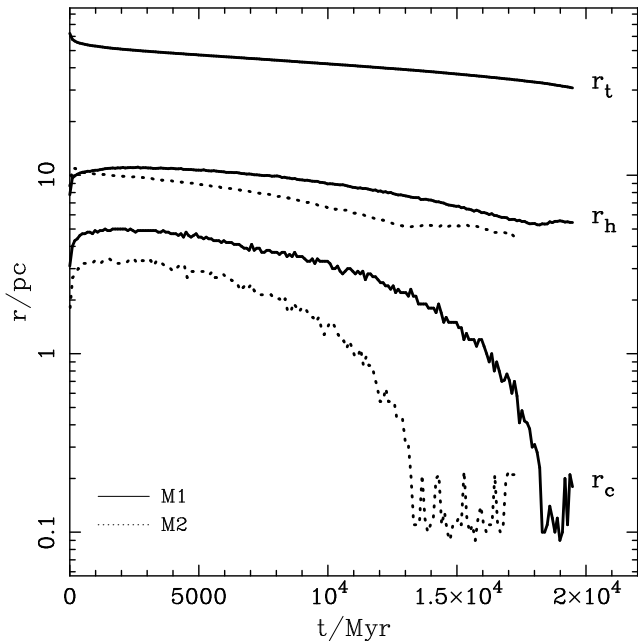


Figure 4. Evolution of the half-mass radius, r_h , and the core-radius, r_c , for the M31 models M1 (solid lines) and M2 (dashed lines). The tidal radius of model M1 is also shown.

towards a similar value of $r_h \simeq 5$ pc even though they start with distinct initial conditions or follow different evolution paths in other respects. The evolution in the $r_c/r_h-r_h/r_t$ plane is also shown for these models in Figure 2d where they all lead to a final $r_h/r_t \simeq 0.18$ and appear to evolve intermediate to the N2 and N3 cases (although for N3 it is not dynamically evolved enough to determine if the path is distinct from M1 or not).

Figure 5 looks at the evolution tracks of our model clusters in the $M-r_h$ plane. We see that for any particular mass the initially extended clusters in the weaker tidal field have the greater half-mass radii. Therefore, clusters at the same R_{gc} in M31 and NGC 6822 will follow distinct paths in the $M-r_h$ plane, assuming they were all close to filling their tidal radii initially. This is to be expected. However, the situation changes if we look at the cluster mass versus r_h/r_t ratio as in Figure 6. Now the tidally-filling clusters in M31 and NGC 6822 follow very similar evolution paths. Küpper, Kroupa & Baumgardt (2008) showed that clusters evolve towards a common post-collapse sequence in this plane. Our models would appear to back this finding (a point we will return to in Section 4) and the sequence in our case corresponds to a constant or slightly increasing r_h/r_t ratio. For models N1 and N2 it is too early to tell if they too will join the sequence when they eventually reach the post-collapse regime but indications are that this is likely.

In Figure 7 we look at how the bound cluster mass changes with cluster age for the various models in this work. We also include the K100-00a and K100-00b models of Hurley (2007) for comparison. As we would expect the clusters in the weaker NGC 6822-like tidal field lose stars/mass at a slower rate compared to clusters orbiting within a galaxy that is ten times more massive. Also, for models M1 and M2 (where M2 is the lower of the dashed lines) we once again see that evolution is more rapid for the $W_0 = 7$ King model

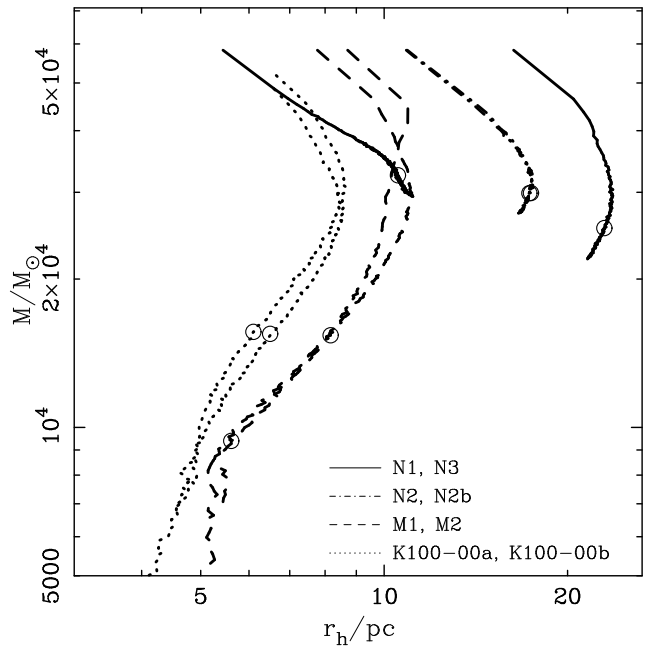


Figure 5. Cluster mass versus half-mass radius for the models in this work as well as models K100-00a and K100-00b of Hurley (2007). For each evolution track the point at 12 Gyr is denoted by an open circle.

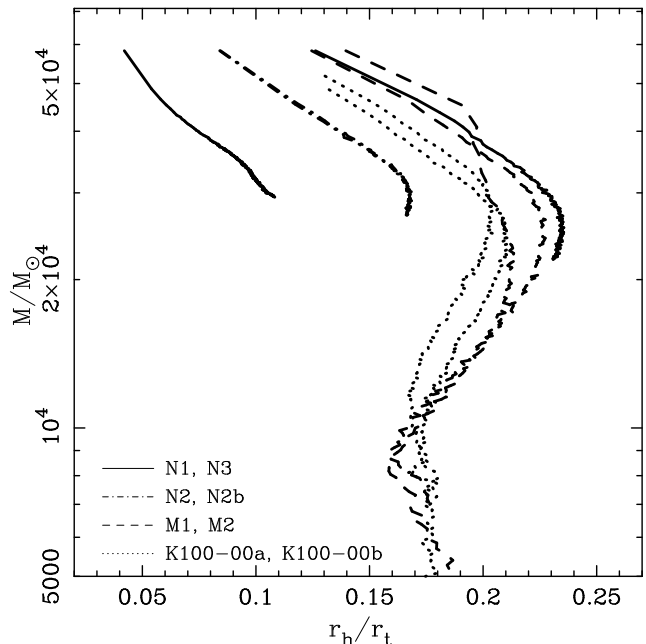


Figure 6. Cluster mass versus the ratio of the half-mass to tidal radius for the models in this work as well as models K100-00a and K100-00b of Hurley (2007).

compared to the Plummer model, although the slopes are similar from about 5 Gyr onwards. For the NGC 6822 model clusters we see that more mass is lost by any particular time if the cluster was initially closer to filling its tidal radius (noting that N1 is the upper of the solid lines). This corresponds to the finding of Gieles & Baumgardt (2008) that clusters that are initially well within the tidal radius

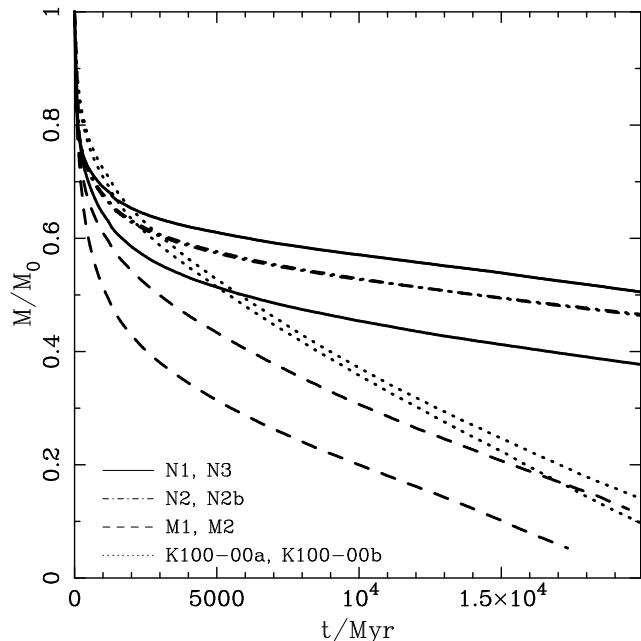


Figure 7. Cluster mass (scaled by the initial mass) as a function of age for the models in this work as well as models K100-00a and K100-00b of Hurley (2007).

take a much greater number of half-mass relaxation times to lose half of their mass than clusters that fill their tidal radius. Following Giersz & Heggie (1997) an expression for the mass-loss rate can be written as:

$$\frac{dM}{dt} \simeq -k_e \frac{M}{t_{rh} \ln \Lambda} \quad (3)$$

where $\ln \Lambda$ is the Coulomb logarithm and we take $\Lambda = 0.4N$. For their N -body models of $N = 500$ stars Giersz & Heggie (1997) found a value of 1.3 for k_e . In Figure 8 we plot k_e as a function of the number of half-mass relaxation times that have elapsed. We see that the behaviour for all of the clusters that initially fill their tidal radii is similar, in particular N3 follows M1, and that k_e decreases as the clusters become more evolved. We also see that k_e is lower for clusters with smaller initial r_h/r_t , a result that is predicted analytically by Gieles & Baumgardt (2008) and previously demonstrated by the Monte Carlo models of Spitzer & Chevalier (1973). In this work we use Eq. 3 and Figure 8 simply as a way of comparing the mass-loss evolution of the various models. A detailed examination of how dissolution times for star clusters in tidal fields can be expected to scale with cluster parameters can be found in Baumgardt & Makino (2003) and Gieles & Baumgardt (2008).

We also remind the reader at this stage that the values of r_h are based on three-dimensional data. If instead we calculated the half-mass radii from a two-dimensional projection a reduction of about 25 per cent would result (Fleck et al. 2006). Furthermore, Hurley (2007) showed that projected half-light radii could be as much as half that of the corresponding half-mass radii for dynamically evolved clusters. In Table 2 we show both the half-light (two dimensional) and half-mass (three-dimensional) radii for the models at an age of 12 Gyr. The errors in both values are also shown. Most obvious is that the errors in $r_{h,1}$ are greater than in

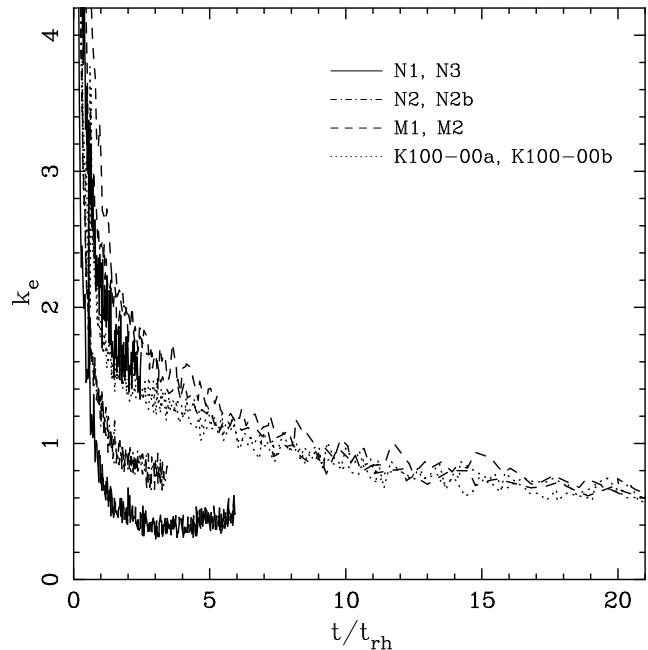


Figure 8. The escape rate (k_e : see text for details) as a function of cluster age (scaled by the half-mass relaxation time) for the models in this work as well as models K100-00a and K100-00b of Hurley (2007).

r_h reflecting that the former quantity fluctuates on a short timescale resulting from a sensitivity to the movement of massive stars in combination with events such as the evolution of bright giants to become dim white dwarfs. We can find particular times when $r_{h,1}$ is as low as 50% that of r_h . However, on average the reduction is in the 30-35% range. It might also be expected that the $r_{h,1}/r_h$ ratio would be smaller for more evolved clusters with a greater degree of mass-segregation (say M1 compared to N3) but overall we see only a weak trend for this.

4 DISCUSSION

We have shown with our model N3 that clusters in the outer regions of a galaxy such as NGC 6822 can naturally evolve to have large half-mass radii provided they begin by filling their tidal radii. The half-light radii in projection can exceed 15 pc which is within the range observed for extended clusters. Furthermore, extended clusters are observed out to ~ 11 kpc in projection from the centre of NGC 6822 which corresponds to a three-dimensional R_{gc} of ~ 15 kpc. Our models were evolved at $R_{gc} = 10$ kpc so following equation 1 we can scale the tidal radius by a factor of 1.5 and potentially the half-mass and half-light radii by a similar factor. Thus half-light radii in excess of 20 pc are possible. Also consider that our models started with $N = 100\,000$ and have a mass of about $30\,000 M_\odot$ remaining at 12 Gyr. If some of the actual clusters are in fact more massive, say twice as massive, then following equation 1 again gives another potential 25% increase in the quoted half-light radii. Therefore, for a dwarf irregular galaxy such as NGC 6822 extended clusters with projected half-light radii in the range 10 – 30 pc can be expected to naturally occur (for a range of masses

and orbits). Such clusters will evolve slowly. They will be dynamically young, having evolved for approximately two half-mass relaxation times, and will not show any signs of core-collapse.

Any clusters in the outer regions of NGC 6822 with half-light radii less than 10 pc will need to have started life relatively compact. Certainly they would not be expected to have filled their tidal radii initially. For a cluster in NGC 6822 to exhibit core-collapse within a Hubble time an initial filling factor of less than 30% is required, or an orbit at R_{gc} much less than 10 kpc. We have shown that for a fixed R_{gc} differences in initial sizes can translate to differences in half-light radii at 12 Gyr by the same factor. We have also shown that primordial binaries do not affect the evolution of the half-mass and half-light radii. This is not surprising for dynamically young clusters and has also been demonstrated for more evolved clusters in stronger tidal fields (Hurley 2007). The internal evolution characteristic that has the most potential to impact the half-light radius evolution is the formation of a central population of BH-BH binaries. Expansion of the half-light radius by this mechanism was shown by Mackey et al. (2008) to start taking effect after one half-mass relaxation time, with the effect increasing to a maximum expansion factor of two by core-collapse (comparing clusters with and without BH-BH binaries). So this could be a mild factor for the most extended clusters in NGC 6822 and potentially play a larger role in determining the observed half-light radii of initially more compact clusters. However, this relies on a source of BHs being retained in the clusters. Overall we find that differences in initial cluster size are the most likely explanation for any measured differences in half-light radii for clusters that otherwise appear similar. The stochastic effect of the presence, or not, of a central population of BH-BH binaries can then possibly play an added role.

Our question of “how do similar clusters obtain different structure?” now seemingly becomes “can clusters be expected to be born with different sizes?”. Baumgardt et al. (2010) asked a similar question after showing that Milky Way GCs beyond R_{gc} of 8 kpc fall into distinct groups of compact, tidally-underfilling clusters and more extended, tidally-filling clusters. They concluded it was more likely that the second group formed with large half-mass radii rather than evolving from a more compact state. Examining the size distribution of globular clusters in a variety of Local Group dwarf galaxies, Da Costa et al. (2009) suggest that there may be two distinct modes of cluster formation with typical half-light radii of 3 and 10 pc, analogous to the findings of Baumgardt et al. (2010). It has been suggested by Ballesteros-Paredes et al. (2009) that tidal forces may play a role in determining the rate at which stars form within molecular clouds, through compression and possible disruption of the clouds. Their calculations show that the resultant star formation efficiency of a particular cloud depends on its position and orientation in the host galaxy. This model is put forward as an alternative to the theory that magnetic field strength and radiative feedback regulate the degree of star formation within a cloud (Price & Bate 2009). Either way, if differences in star formation efficiency can exist between proto-clusters forming in the cores of molecular clouds then Baumgardt & Kroupa (2007) have shown that different r_h/r_t values can result for the bound clusters remaining

after residual gas is expelled. Furthermore, simulations conducted by Elmegreen (2008) have demonstrated that diffuse star clusters can form directly in regions where the background tidal forces are low. Here star formation efficiency is discussed in terms of turbulence (or Mach number) and cloud pressure (or column density). Different combinations produce clusters of different densities with high-pressure regions making the densest clusters while clouds with low density and high Mach numbers give rise to diffuse clusters. The latter are more likely to form in the outer regions of a galaxy where low-density clouds are expected to reside and the diffuse clusters will not be quickly disrupted (Elmegreen 2008). So there are possibilities for variations in environment and/or the properties of molecular clouds producing different star formation efficiencies and a range of r_h/r_t values for young star clusters. What is not immediately clear is whether or not clusters forming in the same environment can have a range of r_h/r_t values owing to variations in cloud properties (size, shape, orientation) alone.

We now turn our focus to the M31 extended cluster system. Our model M1 which started tidally-filling demonstrates the maximum size that a cluster of $M \sim 15\,000 M_\odot$ orbiting at $R_{gc} = 10$ kpc can be expected to have at an age of 12 Gyr. This is not within the extended cluster size range. Of course we are not claiming that our model M1 is a direct representation of a typical star cluster in M31. For a start, the mass of the model is likely to be an underestimate compared to actual M31 clusters. The extended clusters observed in M31 have masses that range from $\sim 10^4$ to $\sim 10^5 M_\odot$ (Huxor et al. 2010a: note that masses for ECs in NGC 6822 are not yet known but are expected to cover a similar range). Thus we have direct models at the lower end of this range but could be as much as a factor of ten too small at the upper end. A factor of ten increase in mass will lead to a larger tidal radius, but only by a factor of two and if the internal radii scale in the same way this gives a projected half-light radius in the range of 10 pc (see Table 2). This is right at the low-end of the extended cluster size range. However, this still does not help when we are looking at two clusters of the same mass (or luminosity) at the same R_{gc} and with very different half-mass radii, as is observed in the inner regions of M31 (Huxor et al. 2010a). Thus it is hard to believe that extended clusters observed in the inner regions of M31, which have half-light radii of about 30 pc, evolved in-situ. It is possible that extended clusters observed in the inner regions are actually further out and only appear in the centre owing to projection effects. Such an effect is not noticeable from the horizontal-branch levels of the few extended clusters that have good colour-magnitude diagrams (Mackey et al. 2006) and if there is a projection effect pushing these clusters into the foreground there is no reason why it shouldn't similarly apply to the compact clusters as well. On the other hand we expect that compact clusters will be more likely to survive in the inner parts of galaxies than extended clusters and radial distributions of GCs in galaxies show that numbers increase towards the centre (see Brodie & Strader 2006, for example). So for compact clusters at least it is reasonable to believe that there is a sizeable population residing in the inner regions of galaxies such as M31, regardless of projection effects.

It is also true that for our models we have used an R_{gc} that for M31 represents only the very inner edge of the

extended cluster locations. As discussed above, and shown by equation 1, in a smooth tidal field the tidal radius of a cluster scales linearly with R_{gc} . So the maximum possible r_h will also increase for clusters observed further out than 10 kpc. The M31 extended clusters are observed out to R_{gc} of 100 kpc and beyond which means a potential factor of ten increase in size for clusters in the outer regions. We note though that other factors such as the relaxation timescale will be affected by a change in cluster size so it is not necessarily a simple case of scaling up a model value at a particular age. To gain some insight we can turn to Mackey & van den Bergh (2005) who have indeed shown a clear trend of increasing r_h with increasing R_{gc} for Milky Way globular clusters (see their figure 9). However, the relation is not linear: going from R_{gc} of 10 to 100 kpc gives a factor of 2 – 3 increase in the typical cluster size (as measured by r_h). If we assume a similar scaling for M31 then we can expect to find clusters with $r_{h,1} \sim 30$ pc in the outer regions. It is particularly interesting to note that the $r_{h,1}$ values derived for the M31 extended clusters (Huxor et al. 2010a) show no obvious correlation with R_{gc} . In combination with our model results this infers that the inner M31 extended clusters either resided at more distant locations for a large part of their lives before moving to their current locations or they were likely accreted as part of one or more dwarf galaxies (perhaps similar in nature to NGC 6822 or the dwarf elliptical Scl-dE1). This latter scenario fits with the picture sketched by Da Costa et al. (2009) where the formation of extended clusters can be expected to be more common in dwarf galaxies where tidal effects are less disruptive and that extended clusters seen in larger galaxies, M31 for example, were accreted in dwarfs that subsequently disrupted. Adding to this argument is evidence of a genuine physical association between the extended clusters (as well as most compact clusters) and coherent stellar streams in the halo of M31 (Mackey et al. 2010).

Our models so far have been evolved within a smooth background potential represented by a point-mass galaxy. This simplification may cause discrepancies when comparing our models to clusters that evolve in host galaxies with distinct structures. In particular, both the Milky Way and M31 exhibit pronounced bulge, disk and halo components which means that the effects of bulge and disk shocking need to be considered. Gnedin, Lee & Ostriker (1999) have demonstrated with Fokker-Planck simulations that gravitational shocks caused by the time-varying tidal forces as clusters pass near the central Galactic bulge or through the Galactic disk can significantly reduce core-collapse and dissolution times. The cluster binding energy is reduced by the shocks so that diffuse clusters are the most susceptible to disruption. However, the effect of the shocks is strongly dependent on the Galactocentric radius. Bulge shocking dominates cluster evolution for R_{gc} of 2 kpc or less (Gnedin & Ostriker 1997) but drops off quickly away from the central nucleus, while disk shocking has a minimal effect for R_{gc} beyond about 8 kpc (Vesperini & Heggie 1997) owing to lower disk density and less frequent passages. To check this we have repeated model M1 using a three-dimensional Galactic potential: a point-mass bulge, a Miyamoto & Nagai (1975) disk (with $a = 4$ kpc and $b = 0.5$ kpc) and a logarithmic halo potential (see Aarseth 2003 and Praagman, Hurley & Power 2010 for the NBODY6 implementation). Masses of 5×10^{10} and

$1.5 \times 10^{10} M_\odot$ were chosen for the bulge and disk, respectively (Xue et al. 2008), with the halo mass chosen so that the mass interior to 10 kpc was the same as for model M1. The cluster was evolved at $R_{gc} = 10$ kpc perpendicular to the disk and there were no obvious changes in evolution of cluster mass or the structural parameters compared to M1. Thus we are confident that our use of a point-mass galaxy has little bearing on our results for clusters evolving at R_{gc} of 10 kpc or greater. Conversely, as suggested by Da Costa et al. (2009), the action of tidal shocks makes it unlikely that extended clusters would be found at smaller galactic radii in large disk galaxies such as M31. A full investigation of the effect of three-dimensional galaxy potentials on the evolution of star clusters will be the focus of future work, noting that the scale-length of the disk of M31 (~ 6 kpc) is larger than for the Milky Way disk (~ 4 kpc: Yin et al. 2009).

Another avenue for future study is the effect of the initial cluster density profile on the subsequent evolution. Trenti, Vesperini & Pasquato (2010) find that King models with different initial concentrations evolve to a similar structural state within a strong tidal field. However, the differences we observed between our models M1 and M2 (evolved in the M31-like tidal field) means that the effect of changing the initial core-density should be investigated for models evolving in a weaker NGC 6822-like tidal field.

We should also note that the results and conclusions we draw regarding extended clusters are based on the assumption that these are essentially normal star clusters where the dynamical processes are not influenced by the presence of any significant dark matter component. If extended clusters are found to contain dark matter then our results to date are not applicable. The only direct constraints on this possibility thus far are the measurements for one M31 extended cluster reported by Collins et al. (2009). Their derived mass-to-light ratio of $M/L = 6.7_{-6.7}^{+15} M_\odot/L_\odot$ rules out very large ratios as seen in most dwarf spheroidals. As stated by Collins et al. (2009) the value is most consistent with a typical star cluster. However, the possibility of M/L as high as 20 still exists so the issue of whether or not extended clusters contain dark matter is yet to be resolved. The case against dark matter is strengthened by Jordi et al. (2009) who measured radial velocities of red giants in Palomar 14, a diffuse GC in the outer regions of the Milky Way, to derive a modest ratio of $M/L \sim 2$. This is compatible with the value expected for a normal stellar initial mass function with no dark matter.

Finally, our models build on a number of important results from previous work regarding general star cluster evolution. A prime example is the work of Küpper, Kroupa & Baumgardt (2008) who used N -body models to demonstrate that post-collapse clusters asymptotically evolve on to a common sequence where the r_h/r_t ratio depends only on the mass remaining in the cluster and not on the initial conditions. They considered open clusters starting with up to $N \simeq 32\,000$ stars and different binary fractions, density distributions, r_h and R_{gc} values. Our models extend this work to include a distribution of stellar masses and stellar evolution for $N = 100\,000$. In doing so we confirm the findings of Küpper, Kroupa & Baumgardt (2008). The common sequence shows a r_h/r_t ratio that starts in the range of 0.15 – 0.2 and increases slightly with decreasing mass. Related to this the same authors found that clusters in a

tidal field show an equilibrium half-mass radius after core-collapse. This was 2 pc for their standard set of models, noting that the particular value will increase for higher initial mass and larger R_{gc} . Our models M1 and M2 have a similar tidal field but larger initial mass. These models also show an equilibrium half-mass radius and as expected it is larger, ~ 5 pc, with the inclusion of stellar evolution likely contributing to some of the increase. This corresponds to a projected half-light radius of about 3 pc which fits with the typical value observed for compact GCs in the Milky Way (Baumgardt et al. 2010) and M31, and indeed almost all galaxies where we see GCs (Da Costa et al. 2009, for example). Of our models in the weaker tidal field only N1 gets close to core-collapse and indeed has a larger half-mass radius at this point, ~ 10 pc, but in this case appears to still be rising.

5 CONCLUSIONS

Using a direct N -body code we have followed the evolution of star clusters with different initial sizes in a tidal field appropriate for a galaxy such as the dwarf irregular NGC 6822 or the Large Magellanic Cloud. We also looked at the effect of increasing the galaxy mass by a factor of ten, appropriate for larger galaxies such as M31 and the Milky Way, on the evolution of clusters which initially fill their tidal radii. Our main findings can be summarised as:

- extended clusters with projected half-light radii of up to 30 pc in galaxies such as NGC 6822 can result from standard star cluster evolution provided that the clusters are close to filling their tidal radii initially;
- internal evolution factors such as the proportion of primordial binaries or the formation of BH-BH binaries do not produce enough expansion so formation as an extended object followed by standard cluster evolution is the most likely path for the extended clusters recently observed;
- observations of clusters of similar mass and age but significantly different half-light radii most likely indicate that the clusters started life filling their tidal radii by different factors;
- in a galaxy with a strong tidal field, such as M31, the maximum half-light radius expected for clusters that evolve at a galactocentric radius of 10 kpc is of the order of 10 pc;
- extended clusters could form naturally in the outer regions of M31 (at ~ 100 kpc) but any extended clusters observed in the inner regions likely formed in one or more dwarf galaxies that were subsequently accreted by M31.

ACKNOWLEDGMENTS

We are indebted to Sverre Aarseth and Keigo Nitadori for creating and maintaining the GPU library for NBODY6. JRH also wishes to thank Ben Barsdell and David Barnes for assistance with GPU usage at Swinburne, as well as Annie Hughes for informative discussions regarding molecular clouds. We also thank the referee for a number of insightful comments.

REFERENCES

- Aarseth S. J., 1999, *PASP*, 111, 1333
- Aarseth S.J., 2003, *Gravitational N-body Simulations: Tools and Algorithms* (Cambridge Monographs on Mathematical Physics). Cambridge University Press, Cambridge
- Aarseth S., Hénon M., Wielen R., 1974, *A&A*, 37, 183
- Ballesteros-Paredes J., Gómez G.C., Loinard L., Torres R.M., Pichardo B., 2009, *MNRAS*, 395, L81
- Baumgardt H., Hut P., Heggie D.C., 2002, *MNRAS*, 336, 1069
- Baumgardt H., Makino J., 2003, *MNRAS*, 340, 227
- Baumgardt H., Makino J., Hut P., 2005, *ApJ*, 620, 238
- Baumgardt H., Kroupa P., 2007, *MNRAS*, 380, 1589
- Baumgardt H., Parmentier G., Gieles M., Vesperini E., 2010, *MNRAS*, 401, 1832
- Binney J., Tremaine S., 1987, *Galactic Dynamics*. Princeton University Press, Princeton
- Brodie J.P., Strader J., 2006, *ARA&A*, 44, 193
- Casertano S., Hut P., 1985, *ApJ*, 298, 80
- Collins M.L.M., Chapman S.C., Irwin M., Ibata R., Martin N.F., Ferguson A.M.N., Huxor A.P., Lewis G.F., Mackey A.D., McConnachie A.W., Tanvir N., 2009, *MNRAS*, 396, 1619
- Da Costa G.S., Grebel E.K., Jerjen H., Rejkuba M., Sharina M.E., 2009, *AJ*, 137, 4361
- de la Fuente Marcos R., 1997, *A&A*, 322, 764
- Duquenooy A., Mayor M., 1991, *A&A*, 248, 485
- Elmegreen B.G., 2008, *ApJ*, 672, 1006
- Fall S.M., Rees M.J., 1977, *MNRAS*, 181, 37
- Fleck J.-J., Boily C.M., Langon A., Deiters S., 2006, *MNRAS*, 369, 1392
- Gao B., Goodman J., Cohn H., Murphy B., 1991, *ApJ*, 370, 567
- Gieles M., Baumgardt H., 2008, *MNRAS*, 389, L28
- Giersz M., Heggie D.C., 1997, *MNRAS*, 286, 709
- Gill M., Trenti M., Miller M.C., van der Marel R., Hamilton D., Stiavelli M., 2008, *ApJ*, 686, 303
- Gnedin O.Y., Ostriker J.P., 1997, *ApJ*, 474, 223
- Gnedin O.Y., Lee H.M., Ostriker J.P., 1999, *ApJ*, 522, 935
- Heggie D.C., 1975, *MNRAS*, 173, 729
- Heggie D.C., Hut P., 2003, *The Gravitational Million Body Problem*. Cambridge University Press, Cambridge
- Hurley J.R., 2007, *MNRAS*, 379, 93
- Hurley J.R., 2008a, *Lecture Notes in Physics*, 760, *The Cambridge N-body Lectures*. Springer-Verlag, Berlin, p. 283
- Hurley J.R., 2008b, *Lecture Notes in Physics*, 760, *The Cambridge N-body Lectures*. Springer-Verlag, Berlin, p. 321
- Hurley J. R., Tout C. A., Aarseth S. J., Pols, O.R., 2004, *MNRAS*, 355, 1207
- Huxor A.P., Tanvir N.R., Irwin M.J., Ibata R., Collett J.L., Ferguson A.M.N., Bridges T., Lewis G.F., 2005, *MNRAS*, 360, 1007
- Huxor A.P., Tanvir N.R., Ferguson A.M.N., Irwin M.J., Ibata R., Bridges T., Lewis G.F., 2008, *MNRAS*, 385, 1989
- Huxor A.P., Ferguson A.M.N., Barker M.K., Tanvir N.R., Irwin M.J., Chapman S.C., Ibata R., Lewis G.F., 2009, *ApJ*, 698, L77
- Huxor A.P., et al., 2010a, *MNRAS*, submitted
- Huxor A.P., et al., 2010b, *MNRAS*, in prep.

- Huxor A.P., et al., 2010c, MNRAS, in prep.
- Hwang N., et al., 2005, in Jerjen H. and Bingelli B., ed, Proceedings of IAU Colloquium 198, Near Field Cosmology with Dwarf Elliptical Galaxies. Cambridge University Press, Cambridge, p. 257
- Jordi K., Grebel E.K., Hilker M., Baumgardt H., Frank M., Kroupa P., Haghi H., Côte P., Djorgovski S.G., 2009, AJ, 137, 4586
- King I.R., 1966, AJ, 71, 64
- Kormendy J., Richstone D., 1995, ARA&A, 33, 581
- Kroupa P., Tout C. A., Gilmore G., 1993, MNRAS, 262, 545
- Küpper A.H.W., Kroupa P., Baumgardt H., 2008, MNRAS, 389, 889
- Mackey A.D., Gilmore G.F., 2004, MNRAS, 355, 504
- Mackey A.D., van den Bergh S., 2005, MNRAS, 360, 631
- Mackey A.D., Huxor A.P., Ferguson A.M.N., Tanvir N.R., Irwin M.J., Ibata R., Bridges T., Johnson R.A., Lewis G.F., 2006, ApJ, 653, L105
- Mackey A.D., Wilkinson M.I., Davies M.B., Gilmore G.F., 2008, MNRAS, 386, 65
- Mackey A.D., Huxor A.P., Ferguson A.M.N., Irwin M.J., Tanvir N.R., McConnachie A.W., Ibata R., Chapman S.C., Lewis G.F., 2010, submitted to ApJ Letters
- Makino J., 2002, in Shara M.M., ed, ASP Conference Series 263, Stellar Collisions, Mergers and their Consequences. ASP, San Francisco, p. 389
- Martin N.F., Ibata R.A., Irwin M.J., Chapman S., Lewis G.F., Ferguson A.M.N., Tanvir N., McConnachie A.W., 2006, MNRAS, 371, 1983
- Miyamoto M., Nagai R., 1975, PASJ, 27, 533
- Mouhcine M., Harris W.E., Ibata R., Rejkuba M., 2010, MNRAS, in press (arXiv:1002.0460)
- Plummer H.C., 1911, MNRAS, 71, 460
- Portegies Zwart S.F., McMillan S.L.W., Hut P., Makino J., 2001, MNRAS, 321, 199
- Praagman A., Hurley J., Power C., 2010, New Astronomy, 15, 46
- Price D.J., Bate M.R., 2009, MNRAS, 398, 33
- Spitzer L.Jr., 1987, Dynamical Evolution of Globular Clusters. Princeton University Press, Princeton
- Spitzer L.Jr., Chevalier R.A., 1973, ApJ, 183, 565
- Stonkuté R., et al., 2008, AJ, 135, 1482
- Tanikawa A., Fukushige T., 2005, PASJ, 57, 155
- Trenti M., Vesperini E., Pasquato M., 2010, ApJ, 708, 1598
- van den Bergh S., Mackey A.D., 2004, MNRAS, 354, 713
- Vesperini E., Heggie D.C., 1997, MNRAS, 289, 898
- Wilkinson M.I., Hurley J.R., Mackey A.D., Gilmore G.F., Tout C.A., 2003, MNRAS, 343, 1025
- Xue X.X., et al., 2008, ApJ, 684, 1143
- Yin J., Hou J.L., Prantzos N., Boissier S., Chang R.X., Shen S.Y., Zhang B., 2009, A&A, 505, 497